

# Self-Assembling Molecular Wires of Halogen-Bridged Platinum Complexes in Organic Media. Mesoscopic Supramolecular Assemblies Consisting of a Mixed Valent Pt(II)/Pt(IV) Complex and Anionic Amphiphiles

Nobuo Kimizuka,\* Noriko Oda, and Toyoki Kunitake

Department of Chemistry and Biochemistry, Graduate School of Engineering, Kyushu University, Fukuoka 812-8581, Japan

Received February 22, 2000

A novel class of supramolecular assemblies in organic media consisting of a molecular wire of a halogen-bridged platinum complex  $[\text{Pt}(\text{en})_2][\text{PtCl}_2(\text{en})_2]^{4+}$  ( $\text{en} = 1,2$ -diaminoethane) and anionic amphiphiles is developed. When double-chained phosphates or sulfonates are employed, the resultant  $[\text{Pt}(\text{en})_2][\text{PtCl}_2(\text{en})_2]^{4+}$ -lipid complexes displayed intervalence charge transfer (CT) absorption bands in the crystalline state. They are soluble in organic solvents because of the amphiphilic superstructure, in which the solvophobic one-dimensional platinum complex is surrounded by solvophilic alkyl chains. CT absorption bands of halogen-bridged linear complexes are maintained in organic media, with varied colors that depend on the chemical structure of constituent amphiphiles. Monoalkylated phosphates failed to form colored, halogen-bridged ternary complexes probably because of their coordination to the axial position of  $\text{Pt}^{\text{II}}(\text{en})_2$ . Formation of mesoscopic supramolecular assemblies in organic media was confirmed for the  $[\text{Pt}(\text{en})_2][\text{PtCl}_2(\text{en})_2]$  complexes by electron microscopy. Interestingly, a supramolecular complex consisting of dihexadecyl sulfosuccinate and  $[\text{Pt}(\text{en})_2][\text{PtCl}_2(\text{en})_2]^{4+}$  displayed clear, indigo solutions that are distinct from the yellow color observed for those of  $[\text{Pt}(\text{en})_2][\text{PtCl}_2(\text{en})_2]$ /dialkyl phosphate complexes. The indigo color of the former complex disappeared upon heating the solution to 60 °C, whereas it reappeared reversibly by cooling the solution to room temperature. In electron microscopy, rodlike nanostructures with a minimum width of 18 nm and lengths of 700–1700 nm were observed after cooling, though not at elevated temperatures. Apparently, the lipid- $[\text{Pt}(\text{en})_2][\text{PtCl}_2(\text{en})_2]^{4+}$  complex undergoes reversible dissociation and reassembly processes in chloroform, and it becomes better dispersed after the reassembling process. The present finding opens a general route to solution chemistry of low-dimensional inorganic complexes and enables rational design and control of self-assembling inorganic molecular wires.

## Introduction

Fabrication and structural control of inorganic low-dimensional materials are one of the central issues in nanochemistry.<sup>1,2</sup> These materials usually exist as basic structural motifs of three-dimensional solids, and their characterization has been conducted for bulk samples. Molecular dispersion of these low-dimensional structures would provide a new class of inorganic nanomaterials that allows us to elucidate physical and chemical properties characteristic of the isolated low-dimensional structure. In addition, rational control of their higher order architecture would be possible by using molecular assembling methodologies such as the Langmuir–Blodgett technique<sup>3</sup> and the layer-by-layer adsorption technique.<sup>4</sup>

A family of pseudo-one-dimensional, halogen-bridged mixed valence complexes  $[\text{Pt}^{\text{II}}(\text{en})_2][\text{Pt}^{\text{IV}}\text{X}_2(\text{en})_2](\text{ClO}_4)_4$  ( $\text{en} = 1,2$ -diaminoethane,  $\text{X} = \text{Cl}, \text{Br},$  or  $\text{I}$ ) belongs to a class II mixed valence complex<sup>5</sup> and are attracting much interest because of

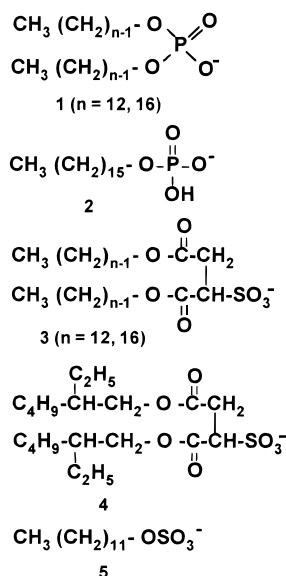
their unique physicochemical properties such as intense intervalence ( $\text{Pt}^{\text{II}}/\text{Pt}^{\text{IV}} \rightarrow \text{Pt}^{\text{III}}/\text{Pt}^{\text{III}}$ ) charge-transfer (CT) absorption,<sup>5–8</sup> semiconductivity,<sup>9</sup> and large third-order nonlinear optical susceptibilities.<sup>10</sup> Unfortunately, these complexes are not soluble in organic media, and when they are dispersed in water, one-dimensional structures in the solid state are disrupted and dissociate into constituent molecular complexes.

Recently, we briefly reported that a mixed valence  $[\text{Pt}^{\text{II}}(\text{en})_2][\text{Pt}^{\text{IV}}\text{Cl}_2(\text{en})_2]$  chain was dispersible in organic media upon formation of polyion complexes with anionic amphiphiles.<sup>11</sup> In this paper, we describe a detailed account of their unique self-assembling characteristics and formation of inorganic molecular wires.

- (5) Robin, M.; Day, P. *Adv. Inorg. Radiochem.* **1967**, *10*, 247–422.
- (6) (a) Kida, S. *Bull. Chem. Soc. Jpn.* **1965**, *38*, 1804. (b) Matsumoto, N.; Yamashita, M.; Kida, S. *Bull. Chem. Soc. Jpn.* **1978**, *51*, 2334–2337. (c) Yamashita, M.; Matsumoto, N.; Kida, S. *Inorg. Chim. Acta.* **1978**, *31*, L381–L382.
- (7) Okamoto, H.; Yamashita, M. *Bull. Chem. Soc. Jpn.* **1998**, *71*, 2023–2039 and references therein.
- (8) Clark, R. J. H. *Chem. Soc. Rev.* **1990**, *19*, 107–131.
- (9) Hamaue, Y.; Aoki, R.; Yamashita, M.; Kida, S. *Inorg. Chim. Acta.* **1981**, *54*, L13–L14.
- (10) Iwasa, Y.; Funatsu, E.; Hasegawa, T.; Koda, T.; Yamashita, M. *Appl. Phys. Lett.* **1991**, *59*, 2219–2221.
- (11) (a) Kimizuka, N.; Oda, N.; Kunitake, T. *Chem. Lett.* **1998**, 695–696. (b) Kimizuka, N.; Sang-Ho, L.; Kunitake, T. *Angew. Chem., Int. Ed. Engl.* **2000**, *39*, 389–391.

- (1) Ozin, G. A. *Adv. Mater.* **1992**, *4*, 612–649.
- (2) Kimizuka, N.; Kunitake, T. *Adv. Mater.* **1996**, *8*, 89–91.
- (3) Kuhn, H. *Physical Methods of Chemistry*; Weissberger, A., Rossiter, B. W., Eds.; Wiley-Interscience: New York, 1972; Vol. 1, Chapter 7, pp 577–702.
- (4) (a) Decher, G. *Science* **1997**, *277*, 1232–1237. (b) Lvov, Y.; Ariga, K.; Onda, M.; Ichinose, I.; Kunitake, T. *Langmuir*, **1997**, *13*, 6195–6203 and references therein.

Chart 1



## Results and Discussion

**Formation of [Pt(en)<sub>2</sub>][PtCl<sub>2</sub>(en)<sub>2</sub>]-Lipid Ternary Complexes and Their Solubility in Organic Media.** When an equimolar mixture of [Pt(en)<sub>2</sub>]Cl<sub>2</sub> and *trans*-[PtCl<sub>2</sub>(en)<sub>2</sub>]Cl<sub>2</sub> was dissolved in deionized water (0.2 mL, [Pt]<sub>total</sub> = 100 mM), the resulting aqueous solution was colorless. The absence of color due to charge-transfer absorption band clearly indicates that Pt<sup>II</sup> and Pt<sup>IV</sup> complexes are molecularly dispersed in water, without formation of a chloro-bridged, mixed valence complex. Addition of aqueous perchloric acid to this mixture results in the formation of red crystals of [Pt(en)<sub>2</sub>][PtCl<sub>2</sub>(en)<sub>2</sub>](ClO<sub>4</sub>)<sub>4</sub>,<sup>6</sup> which is comprised of parallel-aligned infinite chloro-bridged chains of (Pt<sup>II</sup>-Cl-Pt<sup>IV</sup>-Cl)<sub>n</sub>, and ClO<sub>4</sub><sup>-</sup> counteranions are positioned between the mixed valence chains.<sup>6-10</sup>

When aqueous dispersions of amphiphiles **1**–**5** (Na<sup>+</sup> salt) (Chart 1) were added to the aqueous platinum complex at room temperature, yellow precipitates were obtained for **1** and **5**, whereas purple precipitates were obtained for double-chained sulfonates **3**. A branched-chain sulfonate **4** gave only a small amount of colorless precipitates when it was mixed with the aqueous platinum complex at room temperature, but yellow precipitates were obtained when they were mixed at 0 °C. On the other hand, colored precipitates were not formed at any temperature when single-chained phosphate **2** was employed. The colors observed for amphiphiles **1** and **3**–**5** are typical of intervalence charge-transfer (CT; Pt<sup>II</sup>/Pt<sup>IV</sup> → Pt<sup>III</sup>/Pt<sup>III</sup>) absorption of one-dimensional halogen-bridged Pt<sup>II</sup>/Pt<sup>IV</sup> complexes,<sup>6-8</sup> and such a visible absorption band is not present either for [Pt(en)<sub>2</sub>]Cl<sub>2</sub> and *trans*-[PtCl<sub>2</sub>(en)<sub>2</sub>]Cl<sub>2</sub> or for the lipid complexes of [Pt(en)<sub>2</sub>](**1** or **3**)<sub>2</sub> and *trans*-[PtCl<sub>2</sub>(en)<sub>2</sub>](**1** or **3**)<sub>2</sub>. Elemental analysis of these powders indicated the formation of ternary complexes [Pt(en)<sub>2</sub>][PtCl<sub>2</sub>(en)<sub>2</sub>](**1**, **3**, **4**, or **5**)<sub>4</sub> for the colored products. Absence of colored complex formation for the single-chained phosphate **2** might be ascribed to its coordination to [Pt(en)<sub>2</sub>], which interferes with the formation of a chloro-bridged mixed valence complex. Thus, the chemical structure of anionic amphiphiles is crucial for the formation of colored precipitates.

[Pt(en)<sub>2</sub>][PtCl<sub>2</sub>(en)<sub>2</sub>](**1**)<sub>4</sub> (*n* = 12, 16) gave yellow colloidal dispersions in methylcyclohexane. Yellow colloidal dispersions were also obtained for the complex of [Pt(en)<sub>2</sub>][PtCl<sub>2</sub>(en)<sub>2</sub>](**1**)<sub>4</sub> (*n* = 16) and [Pt(en)<sub>2</sub>][PtCl<sub>2</sub>(en)<sub>2</sub>](**5**)<sub>4</sub> in chloroform. On the other hand, short alkyl-chained [Pt(en)<sub>2</sub>][PtCl<sub>2</sub>(en)<sub>2</sub>](**1**)<sub>4</sub> (*n* =

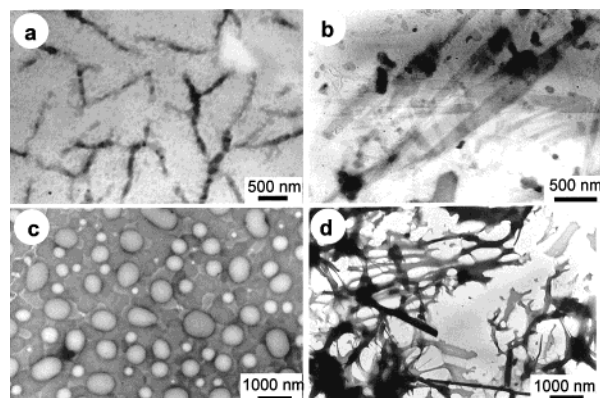


**Figure 1.** Transmission electron micrographs: (a) [Pt(en)<sub>2</sub>][PtCl<sub>2</sub>(en)<sub>2</sub>](**1**)<sub>4</sub> (*n* = 12) in methylcyclohexane, 0.5 mM, poststained with uranyl acetate; (b) [Pt(en)<sub>2</sub>][PtCl<sub>2</sub>(en)<sub>2</sub>](**3**)<sub>4</sub> (*n* = 16) in chloroform, 0.2 mM; (c) [Pt(en)<sub>2</sub>][PtCl<sub>2</sub>(en)<sub>2</sub>](**4**)<sub>4</sub> in chloroform, 1.0 mM; (d) [Pt(en)<sub>2</sub>][PtCl<sub>2</sub>(en)<sub>2</sub>](**5**)<sub>4</sub> in chloroform, 0.5 mM. Samples are not stained.

12) in chloroform displayed only pale-yellow color. This pale color is characteristic of that of noncoordinated *trans*-[PtCl<sub>2</sub>(en)<sub>2</sub>], and therefore, the halogen-bridged coordination structure is not maintained in chloroform in this case. In contrast, [Pt(en)<sub>2</sub>][PtCl<sub>2</sub>(en)<sub>2</sub>](**3**)<sub>4</sub> showed greater solubility and gave clear chloroform solutions with indigo (*n* = 16) or purple color (*n* = 12). Since a mixed-valence inorganic complex of [Pt(en)<sub>2</sub>][PtCl<sub>2</sub>(en)<sub>2</sub>] alone is not soluble in organic media, it is apparent that the solubility is derived from the supramolecular nature of the polyion complexes. In addition, observation of intense yellow, purple, or indigo colors in organic media clearly indicates that one-dimensional mixed valence chains of [Pt(en)<sub>2</sub>][PtCl<sub>2</sub>(en)<sub>2</sub>] remain intact as lipophilic polyion complexes.<sup>11</sup>

**Electron Microscopy.** Figure 1 displays a transmission electron micrograph (TEM) of [Pt(en)<sub>2</sub>][PtCl<sub>2</sub>(en)<sub>2</sub>](**1**)<sub>4</sub> in methylcyclohexane (*n* = 12, 0.5 mM) (part a) and those of [Pt(en)<sub>2</sub>][PtCl<sub>2</sub>(en)<sub>2</sub>](**3**)<sub>4</sub> (*n* = 12, 0.1 mM) (part b), [Pt(en)<sub>2</sub>][PtCl<sub>2</sub>(en)<sub>2</sub>](**4**)<sub>4</sub> (1.0 mM) (part c), and [Pt(en)<sub>2</sub>][PtCl<sub>2</sub>(en)<sub>2</sub>](**5**)<sub>4</sub> (0.5 mM) (part d) in chloroform. These samples are not negatively stained except for [Pt(en)<sub>2</sub>][PtCl<sub>2</sub>(en)<sub>2</sub>](**1**)<sub>4</sub>. [Pt(en)<sub>2</sub>][PtCl<sub>2</sub>(en)<sub>2</sub>](**1**)<sub>4</sub> gives aggregates with rodlike structures in methylcyclohexane (width, ca. 125 nm), whereas fragmented tapes (width, ca. 80–400 nm; length, ca. 200 nm – 2.8 μm) are seen for [Pt(en)<sub>2</sub>][PtCl<sub>2</sub>(en)<sub>2</sub>](**3**)<sub>4</sub> in chloroform. These aggregates are in the mesoscopic dimension (ca. 10 nm to 10 μm), and their morphologies are not very dependent on alkyl chain lengths of **1** and **3**. On the other hand, such aggregate structures are not observable for [Pt(en)<sub>2</sub>][PtCl<sub>2</sub>(en)<sub>2</sub>](**4**)<sub>4</sub>, and instead, unstained circular domains are abundantly seen (Figure 1c). As will be discussed later, the one-dimensional structure of [Pt(en)<sub>2</sub>][PtCl<sub>2</sub>(en)<sub>2</sub>](**4**)<sub>4</sub> is not maintained in chloroform, and these round structures would be produced through dewetting of the solvent during solvent evaporation on the carbon-coated TEM grid. Colloidal dispersion of [Pt(en)<sub>2</sub>][PtCl<sub>2</sub>(en)<sub>2</sub>](**5**)<sub>4</sub> in chloroform displayed irregular structures with both rods (width, ca. 100–450 nm; length, ca. 1–10 μm) and fragmented tapes.

**UV-Visible Spectra of Dispersed Pt<sup>II</sup>-Pt<sup>VI</sup>/Lipid Complexes.** Figure 2 compares absorption spectra of lipid complexes dispersed in chloroform (0.5 unit mM, 20 °C). [Pt(en)<sub>2</sub>][PtCl<sub>2</sub>(en)<sub>2</sub>](**1**)<sub>4</sub> (*n* = 16) gave absorption λ<sub>max</sub> at 460 nm (2.67 eV; ε, 9380 units M<sup>-1</sup> cm<sup>-1</sup>, 1 unit = [Pt(en)<sub>2</sub>][PtCl<sub>2</sub>(en)<sub>2</sub>]), which is close to that observed for the single crystal of [Pt(en)<sub>2</sub>][PtCl<sub>2</sub>(en)<sub>2</sub>](ClO<sub>4</sub>)<sub>4</sub> (λ<sub>max</sub> at 456 nm, 2.72 eV).<sup>12</sup> It is likely that [Pt(en)<sub>2</sub>][PtCl<sub>2</sub>(en)<sub>2</sub>](**1**)<sub>4</sub> dispersed in chloroform possesses a

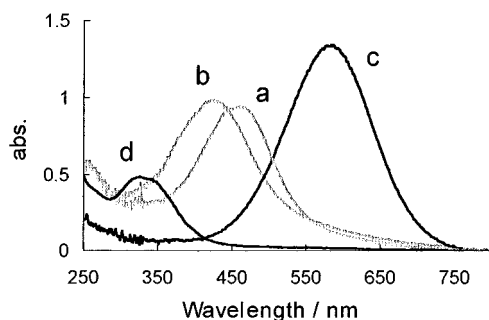


**Figure 2.** UV-vis spectra in chloroform: (a)  $[\text{Pt}(\text{en})_2][\text{Pt}(\text{en})_2(\text{Cl})_2](\mathbf{1})_4$  ( $n = 16$ ), 0.5 mM; (b)  $[\text{Pt}(\text{en})_2][\text{Pt}(\text{en})_2(\text{Cl})_2](\mathbf{5})_4$ , 0.5 mM; (c)  $[\text{Pt}(\text{en})_2][\text{Pt}(\text{en})_2(\text{Cl})_2](\mathbf{3})_4$  ( $n = 16$ ), 0.5 mM; (d)  $[\text{Pt}(\text{en})_2][\text{Pt}(\text{en})_2(\text{Cl})_2](\mathbf{4})_4$ , 2.0 mM. 1 mm cell, 20 °C.

halogen-bridged  $\text{Pt}^{\text{II}}-\text{Pt}^{\text{IV}}$  structure similar to that in  $[\text{Pt}(\text{en})_2][\text{PtCl}_2(\text{en})_2](\text{ClO}_4)_4$  probably because of the structural similarity between the phosphate and  $\text{ClO}_4$  anions.  $[\text{Pt}(\text{en})_2][\text{PtCl}_2(\text{en})_2](\mathbf{5})_4$  showed a blue-shifted  $\lambda_{\text{max}}$  at 420 nm (2.95 eV;  $\epsilon$ , 9810 units  $\text{M}^{-1} \text{cm}^{-1}$ ), while the indigo solution of  $[\text{Pt}(\text{en})_2][\text{PtCl}_2(\text{en})_2](\mathbf{3})_4$  ( $n = 16$ ) gave a much red-shifted absorption band centered at 580 nm (2.15 eV;  $\epsilon$ , 17 900 units  $\text{M}^{-1} \text{cm}^{-1}$ ) with an enhanced molar extinction coefficient. On the other hand,  $[\text{Pt}(\text{en})_2][\text{PtCl}_2(\text{en})_2](\mathbf{4})_4$  showed a considerably weak absorption at 325 nm (2.0 mM sample;  $\epsilon$ , 1220 units  $\text{M}^{-1} \text{cm}^{-1}$ ), and this absorption band is almost identical to that of  $\text{PtCl}_2(\text{en})_2$  in water. Thus, it is reasonable that the chloro-bridged mixed valence chain of  $[\text{Pt}(\text{en})_2][\text{PtCl}_2(\text{en})_2](\mathbf{4})_4$  is not maintained in chloroform, similar to the case of short-chained complex  $[\text{Pt}(\text{en})_2][\text{PtCl}_2(\text{en})_2](\mathbf{1})_4$  ( $n = 12$ ). It seems that regular molecular orientation of unbranched anionic amphiphiles is required to stabilize the extended  $\text{Pt}^{\text{II}}/\text{Pt}^{\text{IV}}$  complex in organic media.

CT exciton energy of halogen-bridged, mixed valence  $\text{Pt}(\text{en})_2$  polymers in the crystalline state has been related to the  $\text{Pt}^{\text{II}}-\text{Pt}^{\text{IV}}$  distance ( $L$ ) in a chain and the energy-gap caused by the lattice distortion, that is, the magnitude of off-center displacement of halogen ions ( $\delta$ ,  $\delta = (I_2 - I_1)/L$  where  $I_1$  and  $I_2$  correspond to the distances of  $\text{Pt}^{\text{VI}}-\text{X}$  and  $\text{Pt}^{\text{II}}-\text{X}$ , respectively).<sup>12</sup> Interplatinum distances ( $L$ ) and off-center displacement ( $\delta$ ) of these complexes vary depending on the bridging halogen ion species (Cl,  $L = 5.403 \text{ \AA}$ ,  $\delta_{\text{Cl}} = 0.142$ ; Br,  $L = 5.493 \text{ \AA}$ ,  $\delta_{\text{Br}} = 0.095$ ; I,  $L = 5.827 \text{ \AA}$ ,  $\delta_{\text{I}} = 0.042$ ).<sup>6c,7</sup> As the  $\text{Pt}^{\text{II}}-\text{Pt}^{\text{VI}}$  distance is increased, the magnitude of off-center displacement is diminished and the CT absorption shows concomitant red shifts.<sup>6c</sup> As the CT absorption of  $[\text{Pt}(\text{en})_2][\text{PtCl}_2(\text{en})_2](\mathbf{3})_4$  in chloroform is maintained in its cast film prepared on a quartz plate, the above relationship would be applicable also to the present solution sample. The observed red shift in CT absorption of  $[\text{Pt}(\text{en})_2][\text{PtCl}_2(\text{en})_2](\mathbf{3})_4$  in chloroform then corresponds to an increase in  $\text{Pt}^{\text{II}}-\text{Pt}^{\text{VI}}$  distance by ca. 0.06  $\text{\AA}$  ( $L \rightleftharpoons 5.46 \text{ \AA}$ ) relative to that of crystalline  $[\text{Pt}(\text{en})_2][\text{PtCl}_2(\text{en})_2](\text{ClO}_4)_4$ . On the other hand, the blue shift observed for  $[\text{Pt}(\text{en})_2][\text{PtCl}_2(\text{en})_2](\mathbf{5})_4$  is indicative of a decrease in  $\text{Pt}^{\text{II}}-\text{Pt}^{\text{VI}}$  distance by ca. 0.02  $\text{\AA}$ .<sup>7,12</sup> These distance changes are small but are well related to sizes of the anionic amphiphiles. The bulkier double-chained sulfonate  $\mathbf{3}$  would tend to increase the  $\text{Pt}^{\text{II}}-\text{Pt}^{\text{VI}}$  distance, while it is slightly shortened by complexation with the single-chained anion  $\mathbf{5}$ .

**Amphiphilic Superstructure Model.** We have previously reported that mesoscopic supramolecular assemblies were formed from amphiphilic complementary hydrogen bond net-

works in organic<sup>13</sup> as well as in aqueous media.<sup>14</sup> In these studies, amphiphilicity played a critical role to direct organization of solvophilic and solvophobic subunits. In the present  $\text{Pt}^{\text{II}}/\text{Pt}^{\text{VI}}$ -lipid system, formation of mesoscopic superstructures indicates that solvophobic one-dimensional  $\text{Pt}^{\text{II}}-\text{Pt}^{\text{VI}}$  complexes are dissolved in organic media with the help of solvophilic alkyl chains of the amphiphiles. Because the width of nanostructures observed in electron microscopy (Figure 1) is larger than bimolecular lengths of the corresponding amphiphiles, we presume that TEM figures consist of bundles of amphiphilic supramolecular polyion complexes in hexagonal (a) or in lamella (b) arrangement as schematically depicted for  $[\text{Pt}(\text{en})_2][\text{PtCl}_2(\text{en})_2](\mathbf{3})_4$  (Figure 3). In these molecular orientations, the divalent cationic charge of one platinum complex is neutralized by negative charges of two anionic amphiphiles that surround the one-dimensional complex. Parts c and d of Figure 3 display schematic CPK packing models of  $[\text{Pt}(\text{en})_2][\text{PtCl}_2(\text{en})_2](\mathbf{3})_4$  ( $n = 16$ ) in the  $yz$  plane (direction of one-dimensional coordination) and in the  $xy$  plane, respectively, as drawn on the basis of the lamella molecular orientation in Figure 3b. A minimum distance between aligned anionic headgroups of double-chained amphiphiles is estimated as ca. 5  $\text{\AA}$  from the CPK molecular model, and this value matches well the  $\text{Pt}^{\text{II}}-\text{Cl}-\text{Pt}^{\text{VI}}$  distance ( $L$ ) in the one-dimensional mixed valence  $[\text{Pt}(\text{en})_2][\text{PtCl}_2(\text{en})_2]$  can be well preserved in the presence of dialkyl amphiphiles.

It is noteworthy that the solubility and spectral characteristics of these complexes in organic media are affected by the chemical structure of amphiphiles. The amphiphiles not only provide solubility in organic media but also exert influence on the intrachain  $\text{Pt}^{\text{II}}-\text{Pt}^{\text{IV}}$  distance and/or on off-center displacement of bridging chloride ions, as revealed by the diverse charge-transfer absorption characteristics. The enhanced solubility of  $[\text{Pt}(\text{en})_2][\text{PtCl}_2(\text{en})_2](\mathbf{3})_4$  compared to the other complexes clearly indicates that the double-chain moiety of sulfosuccinate  $\mathbf{3}$  possesses superior lipophilic nature.

**Temperature Dependence of CT Spectra and Aggregate Morphology.** Thermal characteristics of colored dispersions were investigated. Colloidal dispersion of  $[\text{Pt}(\text{en})_2][\text{PtCl}_2(\text{en})_2](\mathbf{1})_4$  ( $n = 16$ , 0.6 mM) in methylcyclohexane displayed decreases in the CT absorption intensity above 50 °C, and the absorption is totally lost at ca. 60 °C (Figure 4a). When the heated dispersion is cooled to 20 °C, the CT band recovers ca. 50% of the initial intensity (data not shown). A similar thermochromism was observed for  $[\text{Pt}(\text{en})_2][\text{PtCl}_2(\text{en})_2](\mathbf{1})_4$  ( $n = 12$ ) in methylcyclohexane.

The thermochromic behavior of the supramolecular dispersion is more eminent for  $[\text{Pt}(\text{en})_2][\text{PtCl}_2(\text{en})_2](\mathbf{3})_4$  ( $n = 16$ ). When a chloroform solution of  $[\text{Pt}(\text{en})_2][\text{PtCl}_2(\text{en})_2](\mathbf{3})_4$  (0.2 mM) was heated to 45 °C, the absorption intensity at 577 nm started to decrease and it disappeared completely at 60 °C (Figure 4b). Figure 5a shows the temperature dependence of the absorption intensity. The indigo color reappeared reversibly upon cooling. The reappeared spectrum at 20 °C possessed slightly red-shifted absorption maximum at 590 nm, with its intensity amounting to ca. 80% of the unheated, initial dispersion. Obviously, the CT absorption after heating is restored better in this case compared to that observed for  $[\text{Pt}(\text{en})_2][\text{PtCl}_2(\text{en})_2](\mathbf{1})_4$ .

(13) (a) Kimizuka, N.; Kawasaki, T.; Hirata, K.; Kunitake, T. *J. Am. Chem. Soc.* **1995**, *117*, 6360–6361. (b) Kimizuka, N.; Fujikawa, S.; Kuwahara, H.; Kunitake, T.; Marsh, A.; Lehn, J.-M. *J. Chem. Soc., Chem. Commun.* **1995**, 2103–2104.

(14) Kimizuka, N.; Kawasaki, T.; Hirata, K.; Kunitake, T. *J. Am. Chem. Soc.* **1998**, *120*, 4094–4104 and references therein.

(12) Wada, Y.; Mitani, T.; Yamashita, M.; Koda, T. *J. Phys. Soc. Jpn.* **1985**, *54*, 3143–3153.



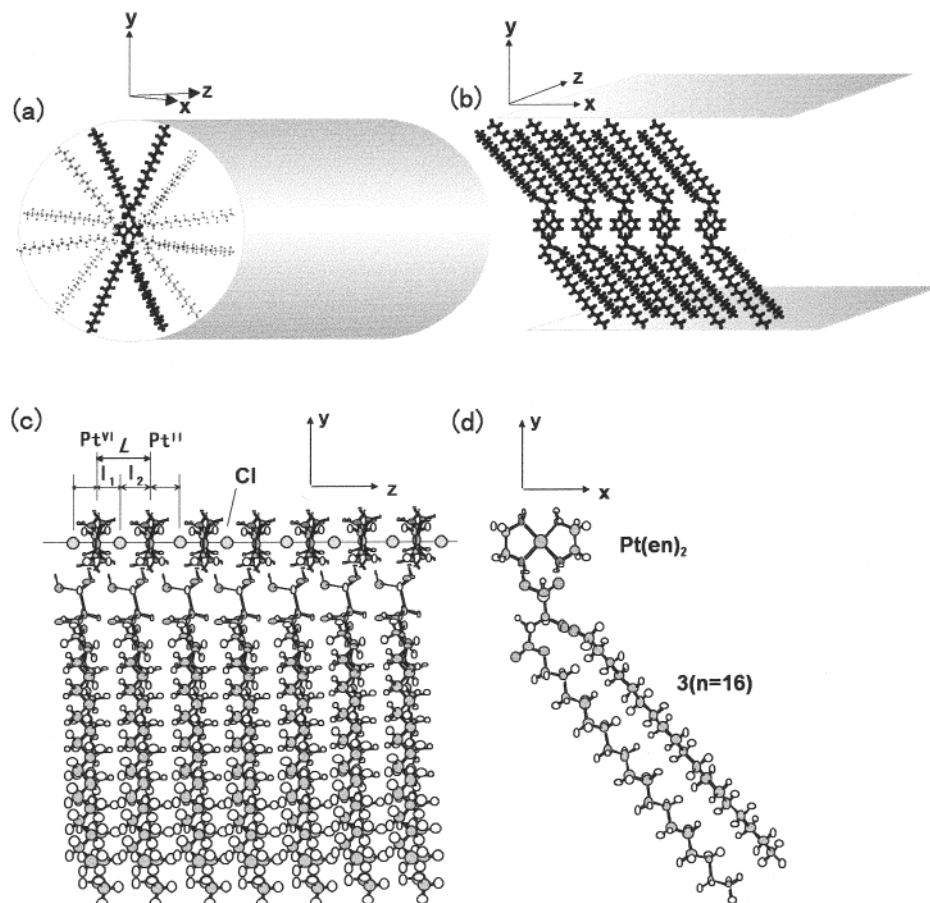


**Figure 3.** Schematic structure model of  $[\text{Pt}(\text{en})_2][\text{Pt}(\text{en})_2(\text{Cl})_2](\mathbf{3})_4$  ( $n = 16$ ): (a) hexagonal model; (b) lamella model; (c) molecular packing in the direction of one-dimensional coordination ( $yz$  plane); (d) molecular orientation model of  $[\text{Pt}(\text{en})_2]$  and  $\mathbf{3}$  in lamella  $xy$  plane.

Figure 5b displays changes in the solution CT absorption intensity with repeated heating and cooling procedures between 25 and 60 °C. It is apparent that the reversible thermochromism is observed for  $[\text{Pt}(\text{en})_2][\text{PtCl}_2(\text{en})_2](\mathbf{3})_4$  and that the peak absorption intensity after the second cooling process is fully restored. Because the CT transition requires the existence of a chloro-bridged extended coordination structure, the observed thermochromism indicates that the one-dimensional complex structure is disrupted at 60 °C, resulting in dissociation into component complexes of  $[\text{Pt}(\text{en})_2](\mathbf{3})_2$  and  $[\text{PtCl}_2(\text{en})_2](\mathbf{3})_2$ . Upon cooling, the dissociated complexes are reassembled and the mixed valence chain is re-formed, resulting in the recovery of CT absorption. The decreased CT spectral intensity in the first heating cycle (ca. 20%, Figure 5b) is indicative of a small change in the coordination structure upon reassembly of  $[\text{Pt}(\text{en})_2][\text{PtCl}_2(\text{en})_2](\mathbf{3})_4$ . This is supported by the morphological transformation of the aggregate structure during this heating cycle, as will be discussed later. On the other hand, the observed recovery of the CT band after heat treatment is much lower for  $[\text{Pt}(\text{en})_2][\text{PtCl}_2(\text{en})_2](\mathbf{1})_4$  (ca. 50%) probably because of coordination of the phosphate headgroup to the dissociated  $\text{Pt}^{\text{II}}(\text{en})_2$ , which hindered re-formation of the halogen-bridged complex.

In the case of  $[\text{Pt}(\text{en})_2][\text{PtCl}_2(\text{en})_2](\mathbf{5})_4$  (0.5 mM in chloroform, Figure 4c), the initial absorption maximum (420 nm at 20 °C) became red-shifted to 442 nm at 40 °C and a further increase in temperature caused a further blue shift to 375 nm (60 °C). The CT absorption did not disappear by heating, and the 375 nm peak at 60 °C was not altered by further cooling the dispersion to 20 °C (data not shown). Thus, subsequent thermochromism was not observed for  $[\text{Pt}(\text{en})_2][\text{PtCl}_2(\text{en})_2](\mathbf{5})_4$ . Its higher crystallinity as inferred from the limited solubility

must have prevented the supramolecular structure from dissociating into the constituent molecular complexes.

The morphology change of  $[\text{Pt}(\text{en})_2][\text{PtCl}_2(\text{en})_2](\mathbf{3})_4$  ( $n = 16$ ) by the heating and cooling treatments was investigated by electron microscopy. When a colorless chloroform solution of  $[\text{Pt}(\text{en})_2][\text{PtCl}_2(\text{en})_2](\mathbf{3})_4$  ( $n = 16$ ), which was heated to 60 °C, was dropped on a carbon-coated TEM grid, crystalline aggregates with widths of 50–200 nm and lengths of 400–550 nm were found in dim, dark domains (Figure 6a). These aggregates are not negatively stained, and such gray domains were not observed for the unheated, indigo dispersion (Figure 1b). Since the 60 °C sample did not show the color of the CT absorption, the extended mixed valence chain is absent in this warm solution. Therefore, the dimly stained domains would consist of dissociated molecular complexes of  $[\text{Pt}(\text{en})_2](\mathbf{3})_2$  and  $[\text{PtCl}_2(\text{en})_2](\mathbf{3})_2$ , whereas the darker aggregates must be generated by crystallization during evaporation of the solution on the grid.

On the other hand, in the case of an indigo dispersion that was obtained upon cooling the 60 °C solution to room temperature, fibrous nanostructures with a minimum width of 18 nm and lengths of 700–1700 nm were abundantly observed (Figure 6b). This morphology is distinct either from that of the irregular aggregates before the heat treatment (Figure 1b) or from that of the heated sample (Figure 6a). Obviously, the ordered nanostructures in Figure 6b must be formed in solution during the cooling process because of reassembly of the dissociated complexes.

In the case of  $[\text{Pt}(\text{en})_2][\text{PtCl}_2(\text{en})_2](\mathbf{1})_4$  ( $n = 12$ ), globular aggregates with diameters of ca. 100–300 nm were observed after cooling the heated methylcyclohexane dispersion to 25 °C

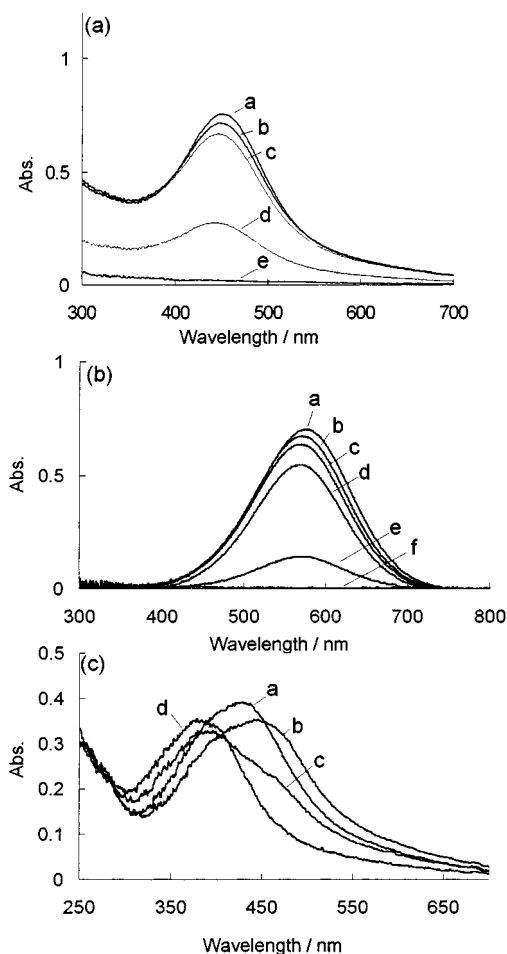


**Figure 4.** Temperature dependence of UV-vis spectra. (a)  $[\text{Pt}(\text{en})_2][\text{Pt}(\text{en})_2(\text{Cl})_2](\mathbf{1})_4$  ( $n = 16$ ), 0.6 mM in methylcyclohexane: a, 20 °C; b, 40 °C; c, 50 °C; d, 55 °C; e, 60 °C. (b)  $[\text{Pt}(\text{en})_2][\text{Pt}(\text{en})_2(\text{Cl})_2](\mathbf{3})_4$  ( $n = 16$ ), 0.2 mM in chloroform: a, 20 °C; b, 40 °C; c, 45 °C; d, 50 °C; e, 55 °C; f, 60 °C. (c)  $[\text{Pt}(\text{en})_2][\text{Pt}(\text{en})_2(\text{Cl})_2](\mathbf{5})_4$ , 0.5 mM in chloroform: a, 20 °C; b, 40 °C; c, 45 °C; d, 60 °C. Cell is 1 mm in length.

(Figure 6c). Thus, the aggregate structure is drastically changed in the case of  $[\text{Pt}(\text{en})_2][\text{PtCl}_2(\text{en})_2](\mathbf{1})_4$ , consistent with the lower recovery of the CT absorption. Analogous globular structures (diameter, ca. 180–560 nm) were observed for a cooled sample of  $[\text{Pt}(\text{en})_2][\text{PtCl}_2(\text{en})_2](\mathbf{5})_4$  in chloroform after the heat treatment (data not shown).

It is interesting that fine fibrous nanostructures are obtained only for  $[\text{Pt}(\text{en})_2][\text{PtCl}_2(\text{en})_2](\mathbf{3})_4$  reassembled upon heat treatment. Because the minimum diameter of the fibrous nanostructure in the electron micrograph is 3 times larger than that estimated for the structure model in Figure 3 (ca. 6 nm), these nanofibers would consist of aggregated lipid-Pt<sup>II</sup>/Pt<sup>IV</sup> polyion complexes.

Figure 7 schematically illustrates the thermal dissociation/reassembly process of the unit supramolecular assembly  $[\text{Pt}(\text{en})_2][\text{PtCl}_2(\text{en})_2](\mathbf{3})_4$ . The chloro-bridged linear Pt<sup>II</sup>/Pt<sup>IV</sup> chain is dispersed as aggregates of the polyion complex with the sulfonate amphiphile, whose lipophilic alkyl chains are oriented toward the organic media. The organized lipid molecules can stabilize the mixed valence chains in solution, leading to dispersion of low-dimensional structures. Upon heating, the linear platinum complex undergoes dissociation into the constituent molecular complexes, while they are reassembled at lower temperatures. The reversible structural transition between

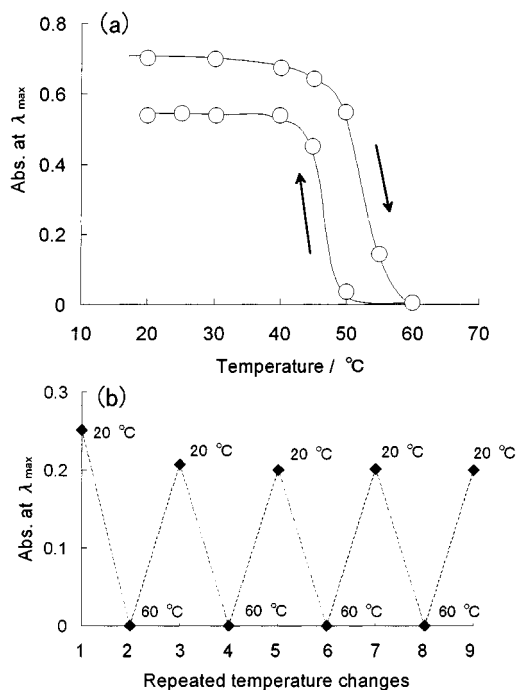


**Figure 5.** (a) Temperature dependence of absorbance at absorption  $\lambda_{\text{max}}$  for  $[\text{Pt}(\text{en})_2][\text{Pt}(\text{en})_2(\text{Cl})_2](\mathbf{3})_4$  ( $n = 16$ ), 0.2 mM, 1 mm cell. (b) Reversibility in the recovery of CT spectra in the course of the repeated temperature changes,  $[\text{Pt}(\text{en})_2][\text{Pt}(\text{en})_2(\text{Cl})_2](\mathbf{3})_4$  ( $n = 16$ ), 0.075 mM, 1 mm cell.

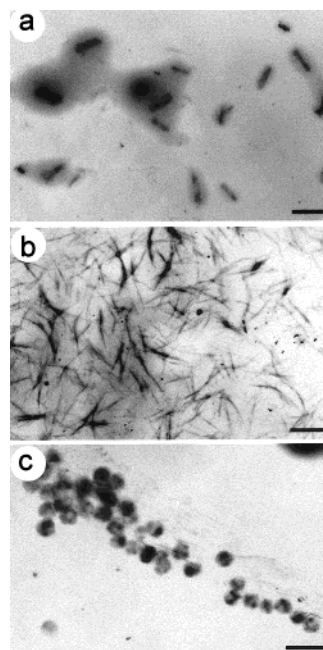


**Figure 6.** Transmission electron micrographs of heated samples: (a)  $[\text{Pt}(\text{en})_2][\text{Pt}(\text{en})_2(\text{Cl})_2](\mathbf{3})_4$  ( $n = 16$ ) dispersed in chloroform (0.1 mM) at 60 °C; (b)  $[\text{Pt}(\text{en})_2][\text{Pt}(\text{en})_2(\text{Cl})_2](\mathbf{3})_4$  ( $n = 16$ ) in chloroform, after cooling to room temperature; (c)  $[\text{Pt}(\text{en})_2][\text{Pt}(\text{en})_2(\text{Cl})_2](\mathbf{1})_4$  ( $n = 12$ ) 0.2 mM in methylcyclohexane, after cooling to room temperature. Samples are not negatively stained. Scale bars represent 1000 nm.

mesoscopic and molecular metal complexes is realized by the self-assembling nature of the amphiphilic supramolecular structure.

## Conclusion

To date, extended linear chains of metal complexes have been restricted to the subject of solid-state chemistry. Such low-

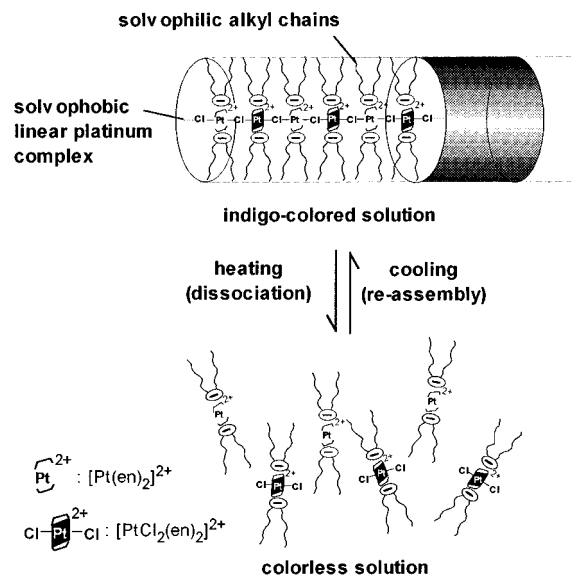


**Figure 7.** Schematic illustration of  $[\text{Pt}(\text{en})_2][\text{Pt}(\text{en})_2(\text{Cl})_2](\mathbf{3})_4$  dispersed in chloroform and its reversible dissociation/reassembly process.

dimensional structures were invariably part of bulk crystals, and rigorous tests of dimensionality have never been achieved.<sup>15</sup> This situation also applies to mixed valence  $\text{Pt}^{\text{II}}/\text{Pt}^{\text{IV}}$  complexes, and their structural modifications in the solid state have been limited to substitution of metal species and replacement of bridging halogen ions, ligands, and counteranions.<sup>6–10,16–17</sup>

In the present results, the extended mixed valence complex was isolated from the three-dimensional solid phase and was shown to maintain its molecular entity in organic media. The self-organization of soluble low-dimensional inorganic nanostructures based on the amphiphilic supramolecular design is of interest in many contexts. First, they provide mesoscopic superstructures that are not obtainable by conventional metal ion directed assembly of oligomeric ligands.<sup>18</sup> Second, in addition to the nanoarchitectural aspect, physicochemical properties of inorganic molecular wires can be tuned by the use of suitably designed amphiphiles. Third, they exhibit reversible self-assembly, which has not been explored for low-dimensional inorganic materials. The present method is straightforward and is widely applicable to preparation of soluble, low-dimensional inorganic materials. The rational design of inorganic molecular wires and regulation of their characteristics are now possible. It allows transformation of solid-state chemistry to solution chemistry and opens the door to “self-assembling” molecular wire research.

- (15) Balch, A. L. In *Extended Linear-Chain Compounds*; Miller, J. S., Eds.; Plenum: New York, 1982; Vol. 1, Chapter 1.
- (16) Matsumoto, N.; Yamashita, M.; Kida, S. *Bull. Chem. Soc. Jpn.* **1978**, *51*, 3514–3518.
- (17) Matsushita, N. Proceedings of the 59th Okazaki Conference, 1997; p 81.
- (18) (a) Lehn, J.-M. *Angew. Chem., Int. Ed. Engl.* **1990**, *29*, 1304–1319. (b) Baxter, P. N. W. In *Comprehensive Supramolecular Chemistry*; Atwood, J. L., Davies, J. E. D., MacNicol, D. D., Vögtle, F., Eds.; Pergamon: Oxford, 1996; Vol. 9, Chapter 5 and references therein. (c) Fujita, M.; Ogura, K. *Bull. Chem. Soc. Jpn.* **1996**, *69*, 1471–1482.

## Experimental Section

**Materials.**  $[\text{Pt}^{\text{II}}(\text{en})_2]\text{Cl}_2$ , *trans*- $[\text{Pt}^{\text{IV}}\text{Cl}_2(\text{en})_2]\text{Cl}_2$ , and  $[\text{Pt}(\text{en})_2][\text{PtCl}_2(\text{en})_2](\text{ClO}_4)_4$  were prepared according to the literature.<sup>19</sup> Amphiphilic phosphates and sulfonates **1–5** were selected as organic counteranions.<sup>11,20</sup> Aqueous dispersions of anionic amphiphiles **1–5** ( $\text{Na}^+$  salt, 20 mM, 2 mL) were added to equimolar solutions containing  $[\text{Pt}(\text{en})_2]\text{Cl}_2$  and *trans*- $[\text{PtCl}_2(\text{en})_2]\text{Cl}_2$  in deionized water (0.2 mL,  $[\text{Pt}]_{\text{total}} = 100$  mM). Yellow precipitates were immediately formed for **1** ( $n = 12$ ). **1** ( $n = 16$ ) afforded colorless precipitates, which turned yellow upon keeping the reaction mixture for a few minutes at 60 °C. **4** afforded yellow precipitates when a 100 mM aqueous solution (0.4 mL) was added to the aqueous platinum complex cooled at 0 °C. Addition of aqueous sodium dodecyl sulfate **5** (80 mM, 0.5 mL) to the Pt complex resulted in formation of yellow precipitates. These precipitates were collected by centrifugation and washed with pure water to remove sodium perchlorate. The samples were then dried in vacuo.

**Elementary Analysis.**  $[\text{Pt}(\text{en})_2][\text{PtCl}_2(\text{en})_2](\mathbf{1})_4$  ( $n = 12$ ). Anal. Calcd for  $\text{C}_{104}\text{H}_{232}\text{O}_{16}\text{N}_8\text{P}_4\text{Pt}_2\text{Cl}_2$ : C, 51.27; H, 9.60; N, 4.60. Found: C, 50.28; H, 9.83; N, 3.90.  $[\text{Pt}(\text{en})_2][\text{PtCl}_2(\text{en})_2](\mathbf{1})_4$  ( $n = 16$ ). Anal. Calcd for  $\text{C}_{136}\text{H}_{296}\text{O}_{16}\text{N}_8\text{P}_4\text{Pt}_2\text{Cl}_2$ : C, 56.62; H, 9.22; N, 3.89. Found: C, 55.03; H, 10.39; N, 3.72.  $[\text{Pt}(\text{en})_2][\text{PtCl}_2(\text{en})_2](\mathbf{3})_4$  ( $n = 12$ ). Anal. Calcd for  $\text{C}_{120}\text{H}_{244}\text{O}_{28}\text{N}_8\text{S}_4\text{Pt}_2\text{Cl}_2$ : C, 50.81; H, 8.67; N, 3.95. Found: C, 49.99; H, 8.62; N, 3.90.  $[\text{Pt}(\text{en})_2][\text{PtCl}_2(\text{en})_2](\mathbf{3})_4$  ( $n = 16$ ). Anal. Calcd for  $\text{C}_{152}\text{H}_{308}\text{O}_{28}\text{N}_8\text{S}_4\text{Pt}_2\text{Cl}_2$ : C, 55.56; H, 9.45; N, 3.41. Found: C, 55.09; H, 9.52; N, 3.37.  $[\text{Pt}(\text{en})_2][\text{PtCl}_2(\text{en})_2](\mathbf{4})_4$ . Anal. Calcd for  $\text{C}_{88}\text{H}_{180}\text{O}_{16}\text{N}_8\text{S}_4\text{Pt}_2\text{Cl}_2$ : C, 44.26; H, 7.60; N, 4.69. Found: C, 43.79; H, 7.56; N, 4.58.  $[\text{Pt}(\text{en})_2][\text{PtCl}_2(\text{en})_2](\mathbf{5})_4$ . Anal. Calcd for  $\text{C}_{56}\text{H}_{132}\text{O}_{16}\text{N}_8\text{S}_4\text{Pt}_2\text{Cl}_2$ : C, 38.15; H, 7.55; N, 6.36. Found: C, 37.56; H, 7.46; N, 6.14. The colored complexes were placed in 1 mL of chloroform or 1 mL of methylcyclohexane, and dispersions of ca. 1 unit mM were prepared by ultrasonication (Branson Sonifier 5210).

**Measurements.** UV–vis spectra are recorded on a JASCO V-570. Transmission electron microscopy (TEM) was conducted on a Hitachi H-600 instrument. Samples were prepared by placing a drop of chloroform or methylcyclohexane solution on a carbon-coated TEM grid on a filter paper. The drops immediately penetrated into the filter paper, and the grids dried in air were observed without staining or by the negative poststaining method (uranyl acetate).

**Acknowledgment.** The authors are grateful to Dr. S. Fujikawa for his experimental assistance and to Prof. M. Yamashita (Tokyo Metropolitan University) for helpful discussions. This work was supported by a Grant-in-Aid for COE Research “Design and Control of Advanced Molecular Assembly Systems” (No. 08CE2005), by a Grant-in-Aid for Scientific Research on Priority Areas “Metal-Assembled Complexes” (No. 11136237) from the Ministry of Education, Science, Culture and Sports, Japan, and by The Fukuoka Industry, Science and Technology Foundation.

**Supporting Information Available:** Atomic force microscopy (AFM) image of  $[\text{Pt}(\text{en})_2][\text{Pt}(\text{en})_2(\text{Cl})_2](\mathbf{3})_4$  ( $n = 16$ ) cast on a mica surface and its height profile. This material is available free of charge via the Internet at <http://pubs.acs.org>.

IC000189F

- (19) Basolo, F.; Bailar, J. C.; Tarr, B. R. *J. Am. Chem. Soc.* **1950**, *72*, 2433–2438.
- (20) Kunitake, T.; Okahata, Y. *Bull. Chem. Soc. Jpn.* **1978**, *51*, 1877–1879.